

Low-temperature conductive tip atomic force microscope for carbon nanotube probing and manipulation

M. Prior, A. Makarovski, and G. Finkelstein^{a)}

Department of Physics, Duke University, Durham, North Carolina 27708

(Received 24 January 2007; accepted 26 June 2007; published online 1 August 2007)

The authors describe conductive tip atomic force microscope used for imaging carbon nanotubes at low temperatures. The instrument allows them to measure the tip-nanotube conductance while performing the topographic scan of the nanotubes on a *nonconductive* SiO₂ substrate. For nanotubes weakly coupled to the contacting electrode, they observe the Coulomb blockade pattern in the tip-nanotube conductance. They reversibly modified the conductance pattern by applying the tip pressure. © 2007 American Institute of Physics. [DOI: 10.1063/1.2759986]

Cryogenic scanning probe techniques offer unique possibilities to probe quantum effects in nanostructures. In particular, the local electronic properties of carbon nanotubes have been investigated at low temperatures by a number of scanning techniques.^{1–6} In some of these works, the nanotubes were deposited on conducting substrates, and the conductance along the nanotube is shunted by the substrate. In a few notable exceptions, nanotubes had separate contacts along the length, allowing for simultaneous conductance measurements at low temperature. In Refs. 6 and 7, scanned gate microscopy and frequency shift microscopy were used to study the Coulomb blockade in nanotubes. In Refs. 8 and 9 a scanning tunneling microscope was used to tunnel into suspended nanotubes.

In this work we use the low-temperature conductive tip atomic force microscope (AFM) to probe carbon nanotubes grown on a nonconductive SiO₂ layer. We can measure the tip-nanotube conductance while performing the topographic scan of the nanotubes. We observe the Coulomb blockade effect in the tunneling spectrum of nanotubes weakly coupled to the contact lead. We reversibly modify the conductance pattern by pushing the AFM tip into the nanotube. In the following, we first describe our microscope and the scanning technique, then demonstrate the nanotube conductance imaging, and finally discuss the tip-nanotube conductance measurements.

Our microscope is designed for low-temperature operation inside a cryostat with a 1.25 in. bore. Scanning motion and coarse positioning in the microscope are accomplished using an inertial slider based on the Besocke design.¹⁰ In our microscope, the tip and the AFM sensor are moved during the initial coarse positioning, and then remain stationary while the sample is scanned. The AFM sensor is made up of a platinum/iridium tip mounted on a commercial quartz tuning fork. This assembly is in turn mounted on a dithering piezoplate.¹¹ The tip is glued to the tuning fork in such a way that there is no conduction between the tip and the tuning fork electrodes. To measure the local conductance, a gold wire is attached to the tip using a conductive epoxy. To avoid damping the oscillations of the quartz tuning fork, we use a wire of 25 μm in diameter. As a result, we obtain a resonance with a *Q* factor of several hundreds at room temperature and over a thousand at low temperature in He exchange

gas. We use a homemade frequency detection system to monitor the changes in the frequency of the tuning fork sensor, which is forced to oscillate at its natural resonance frequency. The frequency shift observed when the tip interacts with the surface is used as a feedback signal,¹¹ which is sent to a commercial scanning controller and data acquisition system (RHK Technology).

We maintain a distance from the surface by keeping a frequency shift of the tuning fork at about +1 Hz. We have chosen this frequency shift as it gives us the best mix of topography and conductivity information while maintaining the sharpness of the tip. We use an “intermittent contact” scanning method: the sample to tip distance is kept small, so that during each oscillation the tip approaches the surface close enough to produce a measurable current. Therefore, we can record conductivity information while we scan the surface. This method was introduced in Refs. 12–14 to study carbon nanotubes at room temperature.

An example of conductance scanning can be seen in Fig. 1, where we image a palladium/gold comb-shaped electrode deposited on insulating SiO₂. The base of the comb is biased (typically ~10 mV), and the current signal is observed only when the tip is positioned above the metal. Some of the stripes in the comb pattern are broken along the length and do not show up in the conductance image.

We study single-wall carbon nanotubes with diameters of around 2 nm grown on a Si/SiO₂ substrate by a chemical vapor deposition method described in Ref. 15. To pattern the sample, we use deep UV photolithography with a MMA/PMMA (methacrylic acid/polymethyl methacrylate) bilayer resist. A 20 nm layer of palladium/gold is thermally evaporated on the surface in a shape of square grid with a 7 μm pitch. The grid consists of 5 μm open square windows sepa-

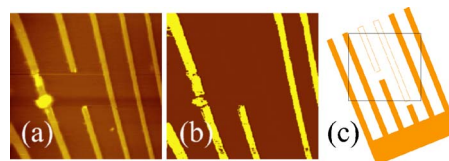


FIG. 1. (Color online) Simultaneous $25 \times 25 \mu\text{m}^2$ topography (a) and conductance (b) scans of a SiO₂ surface with a comb-shaped Pd/Au electrode [schematics in (c)]. The schematic drawing shows that some of the metal lines have breaks and are electrically disconnected from the rest of the pattern (open rectangles). These lines disappear from the conductance scan (indicated by the square window in the schematics).

^{a)}Electronic mail: gfeb@phy.duke.edu

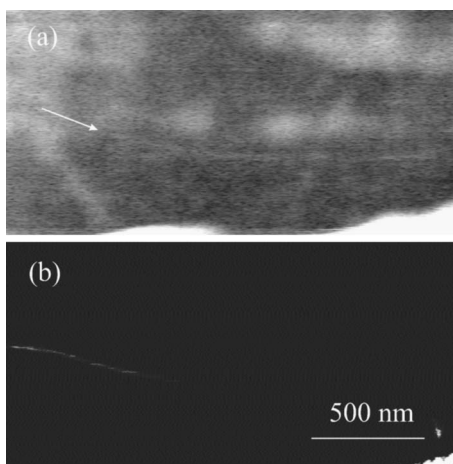


FIG. 2. (a) Topography and (b) conductance images of the same $2 \times 1 \mu\text{m}^2$ region of the SiO_2 surface with a nearby metal grid (bottom right corner of the images). Several nanotubes are visible as bright lines in (a), but most of them are not conductive. The nanotube that is found to be conductive in (b) is marked by an arrow in (a). Its diameter is about 1 nm. Temperature: 5 K.

rated by $2 \mu\text{m}$ wide metal lines. The nanotubes are long enough, so that most of them are contacted by the metal grid.

After cooling down to low temperatures and coarse tip approach, we carry out a topographic as well as a conductive scan to find nanotubes that are well connected to the metal grid. Figure 2 demonstrates the topographic and conductance images of a region covered with several nanotubes (bright lines in the topographic image). However, most of them do not show up in the conductance image, indicating either their weak coupling to the metal grid, or low intrinsic conductance. The nanotube that demonstrates significant conductance in Fig. 2(b) is marked by an arrow on the topographic image.

We now can position the tip on top of the nanotube, turn off the AFM feedback (and the tuning fork oscillation) and measure the local spectroscopic information [schematic in Fig. 3(a)]. Several of the studied nanotubes have demonstrated Coulomb blockade pattern in their tip-sample conductance spectra. In Fig. 3(b), we present the tip-nanotube differential conductance as a function of the tip dc bias and the back gate voltage. Several “Coulomb diamonds” (see Ref. 16

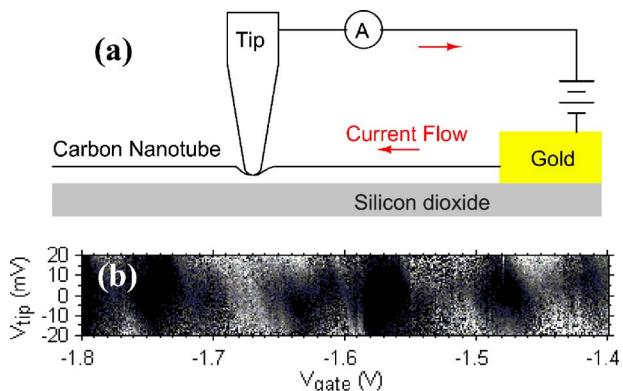


FIG. 3. (Color online) Tip-nanotube conductance in the Coulomb blockade regime. (a) Schematic: AFM tip pushing into a nanotube. Nanotube-tip conductance is simultaneously monitored. (b) Conductance measured as a function of the voltage applied to the back gate (Si/SiO₂ substrate) and the tip-sample bias presented as a gray scale map. Higher conductance appears bright. Temperature: 5 K.

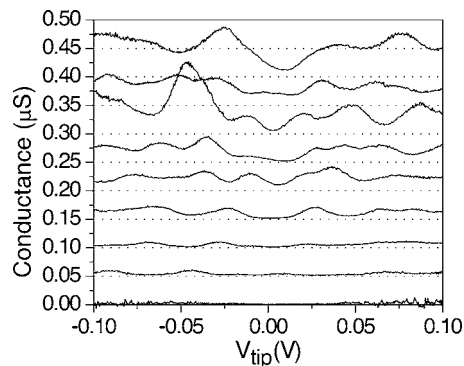


FIG. 4. Conductance of another nanotube sample. Several curves are shown corresponding to the tip pushing stronger into the nanotube (top to bottom). The individual curves are offset by 50 nS. Temperature: 5 K.

for a review) are visible. The charging energy extracted from the vertical scale of the diamonds is too large to be explained by the charge quantization in the nanotube segment between the tip and the contact electrode. We therefore conclude that the nanotube has a break (weak link) along its length.

Figure 4 shows the tip-nanotube conductance measured as a function of the tip bias on a different nanotube. We tentatively attribute the conductance oscillations found in Fig. 4 to the Coulomb blockade. By pushing the tip harder into the nanotube, we observe an overall increase of conductance. This behavior is reasonable, since the conductance is likely limited by the interface between the nanotube and the tip. Also, we observe that the conductance pattern shifts as the tip is pushed further into the nanotube. (Notice, for example, that the conductance curves in Fig. 4 demonstrate either a zero-bias peak or a valley, depending on the tip position.) Finally, the observed modification of conductance is reversible, and the conductance curves are reproduced when the tip is returned to the original location.

In conclusion, we describe a low-temperature conductive tip AFM, which is capable of local conductance imaging of carbon nanotubes. This instrument allows us to find individual nanotubes on the sample surface and obtain the local spectroscopic information. We observe the Coulomb blockade in the tip-nanotube conductance. We also find that the pressure induced by the scanning tip reversibly modifies the conductance pattern. This observation suggests the possibility of using nanotubes as low-temperature electromechanical sensors.

The authors thank J. Liu for providing facilities to grow the carbon nanotube samples. The work is supported by NSF (DMR-0239748).

¹T. W. Odom, J. L. Huang, P. Kim, and C. M. Lieber, *Nature (London)* **391**, 62 (1998).

²M. Ouyang, J. L. Huang, C. L. Cheung, and C. M. Lieber, *Science* **292**, 702 (2001).

³J. W. G. Wildoer, L. C. Venema, A. G. Rinzler, R. E. Smalley, and C. Dekker, *Nature (London)* **391**, 59 (1998).

⁴L. C. Venema, J. W. G. Wildoer, J. W. Janssen, S. J. Tans, H. L. J. T. Tuinstra, L. P. Kouwenhoven, and C. Dekker, *Science* **283**, 52 (1999).

⁵S. G. Lemay, J. W. Janssen, M. van den Hout, M. Mooij, M. J. Bronikowski, P. A. Willis, R. E. Smalley, L. P. Kouwenhoven, and C. Dekker, *Nature (London)* **412**, 617 (2001).

⁶M. T. Woodside and P. L. McEuen, *Science* **296**, 1098 (2002).

⁷J. Zhu, M. Brink, and P. L. McEuen, *Appl. Phys. Lett.* **87**, 242102 (2005).

⁸B. J. LeRoy, S. G. Lemay, J. Kong, and C. Dekker, *Nature (London)* **432**, 371 (2004).

- ⁹B. J. LeRoy, J. Kong, V. K. Pahilwani, C. Dekker, and S. G. Lemay, *Phys. Rev. B* **72**, 075413 (2005).
- ¹⁰K. Besocke, *Surf. Sci.* **181**, 1450039 (1987).
- ¹¹F. J. Giessibl, *Rev. Mod. Phys.* **75**, 949 (2003).
- ¹²M. Stadermann, H. Grube, J. J. Boland, S. J. Papadakis, M. R. Falvo, R. Superfine, and S. Washburn, *Rev. Sci. Instrum.* **74**, 3653 (2003).
- ¹³M. Stadermann, S. J. Papadakis, M. R. Falvo, Q. Fu, J. Liu, Y. Fridman, J. J. Boland, R. Superfine, and S. Washburn, *Phys. Rev. B* **72**, 245406 (2005).
- ¹⁴M. Stadermann, S. J. Papadakis, M. R. Falvo, J. Novak, E. Snow, Q. Fu, J. Liu, Y. Fridman, J. J. Boland, R. Superfine, and S. Washburn, *Phys. Rev. B* **69**, 201402 (2004).
- ¹⁵B. Zheng, C. G. Lu, G. Gu, A. Makarovski, G. Finkelstein, and J. Liu, *Nano Lett.* **2**, 895 (2002).
- ¹⁶L. P. Kouwenhoven, C. M. Marcus, P. L. McEuen, S. Tarucha, R. M. Westervelt, and N. S. Wingreen, in *Mesoscopic Electron Transport*, edited by L. L. Sohn, L. P. Kouwenhoven, and G. Schon (Kluwer Academic, Boston, 1997), E345, pp. 105.